

Spurious Resonances for Substructured FEM-BEM Coupling

Antonin Boisneault^[0000-0001-7986-9048],
Marcella Bonazzoli^[0000-0002-0284-5643],
Xavier Claeys^[0000-0003-0826-6244],
Pierre Marchand^[0000-0002-2522-6837]

1 Introduction and definition of the problem

When solving the Helmholtz equation in complex heterogeneous media, it is of interest to decompose the domain according to the variation of the wavenumber. Local problems in homogeneous subdomains can be reformulated as equations set on their boundary, and the global problem is solved with Finite Element Method - Boundary Element Method (FEM-BEM) coupling techniques [4, 6]. Recently, a substructured formulation, called *Generalized Optimized Schwarz Method (GOSM)*, has been designed for bounded domains, with weakly imposed boundary conditions, see [3], and extended in [1] to unbounded domains and interface conditions arising from several FEM-BEM coupling techniques. Unfortunately, FEM-BEM variational formulations can be ill-posed for certain wavenumbers called *spurious resonances* [11]. The combined FEM-BEM formulations from [5] eliminate the spurious resonances, but rely on a compact regularizing operator and their numerical implementation might be complicated. In this paper, we choose to focus on the classical Johnson-Nédélec [6] and Costabel [4] couplings and show that also the associated GOSMs suffer from the same spurious resonances. For both couplings, we give an explicit expression of

Antonin Boisneault
POEMS, CNRS, Inria, ENSTA, Institut Polytechnique de Paris, 91120 Palaiseau, France, Inria,
Unité de Mathématiques Appliquées, ENSTA, Institut Polytechnique de Paris, 91120 Palaiseau,
France, e-mail: antonin.boisneault@inria.fr

Marcella Bonazzoli
Inria, Unité de Mathématiques Appliquées, ENSTA, Institut Polytechnique de Paris, 91120
Palaiseau, France, e-mail: marcella.bonazzoli@inria.fr

Xavier Claeys
POEMS, CNRS, Inria, ENSTA, Institut Polytechnique de Paris, 91120 Palaiseau, France, e-mail:
xavier.claeys@ensta.fr

Pierre Marchand
POEMS, CNRS, Inria, ENSTA, Institut Polytechnique de Paris, 91120 Palaiseau, France, e-mail:
pierre.marchand@ensta.fr

the kernel of the local operator associated with the interface between the FEM and BEM subdomains. This kernel and the one of the corresponding classical FEM-BEM couplings are simultaneously non-trivial.

For simplicity, we consider a three subdomains configuration. The impenetrable obstacle $\Omega_O \subset \mathbb{R}^d$ ($d = 2, 3$) is assumed connected Lipschitz bounded, with a connected complement $\Omega := \mathbb{R}^d \setminus \overline{\Omega_O}$ decomposed into two connected Lipschitz subdomains: Ω_F bounded with $\partial\Omega_O \subseteq \partial\Omega_F$ and Ω_B unbounded with bounded boundary, satisfying $\Omega_F \cap \Omega_B = \emptyset$ (see Figure 1). We are interested in solving the following Helmholtz problem, which models time-harmonic acoustic wave propagation: find $u \in H_{\text{loc}}^1(\Delta, \Omega)$ such that

$$\begin{cases} -\Delta u - \kappa^2 u = f, & \text{in } \Omega, \\ \text{boundary condition on } \partial\Omega, \\ \text{Sommerfeld's radiation condition,} \end{cases} \quad (1)$$

where the wavenumber $\kappa: \Omega \rightarrow \mathbb{R}_{>0}$ is constant in Ω_B and $f \in L^2(\Omega_F)$. See [10, Def. 2.6.1] for the definition of $H_{\text{loc}}^1(\Delta, \Omega)$, and [8, Sect. 2.2] for the Sommerfeld's radiation condition. Boundary conditions can be of Dirichlet, Neumann, Robin, or even mixed type, so Ω_O can represent an impenetrable obstacle with a sound-soft or sound-hard boundary, for instance.

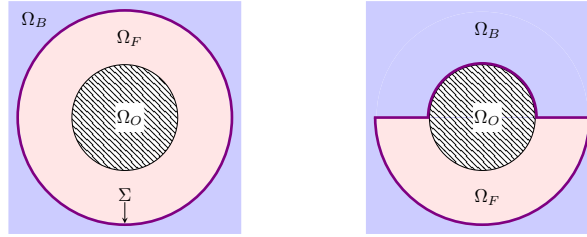


Fig. 1 Example of allowed (left) and forbidden (right) geometries (for simplicity).

In FEM-BEM coupling, the FEM is used for the (possibly) heterogeneous subdomain Ω_F , the BEM is applied for the homogeneous domain Ω_B , and transmission conditions are imposed at the interface $\Sigma := \partial\Omega_F \cap \partial\Omega_B$. Our FEM-BEM formulation, based on the *Generalized Optimized Schwarz Method* (GOSM) [1, 3], is set on Σ and reads:

$$(\text{Id} + \Pi \text{S})(q_B, q_F) = \mathbf{rhs}, \quad (2)$$

where Π is a (possibly) non-local exchange operator, $\text{S} := \text{diag}(\text{S}_B, \text{S}_F)$ is a block-diagonal scattering operator and $q_B, q_F \in H^{-1/2}(\Sigma)$ are outgoing impedance traces shared between Ω_B and Ω_F . More details about (2) can be found in [3, Prop. 8.1]. To derive the substructured formulation (2), first we write Problem (1) in variational form: Find $u \in H^1(\Omega_F)$, $p \in H^{-1/2}(\Sigma)$, such that $\forall v \in H^1(\Omega_F)$, $\forall q \in H^{-1/2}(\Sigma)$,

$$\int_{\Omega_F} (\nabla u \cdot \nabla v - \kappa^2 uv) \, dx + \langle A_\Sigma(u|_\Sigma, p), (v|_\Sigma, q) \rangle = \ell(v), \quad (3)$$

where the explicit expression of $A_\Sigma: H^{1/2}(\Sigma) \times H^{-1/2}(\Sigma) \rightarrow H^{-1/2}(\Sigma) \times H^{1/2}(\Sigma)$ depends on the choice of the FEM-BEM coupling and involves Boundary Integral Operators (BIOs) (see Section 2). The linear form ℓ accounts for the contributions of the source term f and the boundary condition on Ω_O . For instance, $\ell(v) = \int_{\Omega_F} f v \, dx$ for homogeneous Neumann boundary condition, or if $\Omega_O = \emptyset$. Here, the canonical duality pairing between a Banach space H and its topological dual H^* is denoted $\langle \cdot, \cdot \rangle: H^* \times H \rightarrow \mathbb{C}$ and defined by $\langle \varphi, v \rangle := \varphi(v)$. We emphasize that the duality pairings we consider do *not* involve any complex conjugation.

Next, we introduce a boundary operator $B_\Sigma: H^{1/2}(\Sigma) \times H^{-1/2}(\Sigma) \rightarrow H^{1/2}(\Sigma)$, defined by $B_\Sigma(\phi, p) := \phi$, and also consider a *transmission* (or *impedance*) operator $T_\Sigma: H^{1/2}(\Sigma) \rightarrow H^{-1/2}(\Sigma)$, satisfying $\langle T_\Sigma(\phi), \bar{\phi} \rangle > 0 \quad \forall \phi \in H^{1/2}(\Sigma) \setminus \{0\}$, $T_\Sigma^* = T_\Sigma$, and $\text{Re}(T_\Sigma) > 0$. The scattering operator S_B involved in the GOSM is given by $\text{Id} + 2\iota T_\Sigma B_\Sigma (A_\Sigma - \iota B_\Sigma^* T_\Sigma B_\Sigma)^{-1} B_\Sigma^*$, see [3, Prop. 7.2]. We aim to study the kernel of $A_\Sigma - \iota B_\Sigma^* T_\Sigma B_\Sigma$, which is crucial to establishing the well-posedness of the GOSM.

2 Boundary integral operators and kernel of $A_\Sigma - \iota B_\Sigma^* T_\Sigma B_\Sigma$

The *Dirichlet-Neumann trace map* on Σ (from Ω_B), $\gamma: H_{\text{loc}}^1(\Delta, \overline{\Omega_B}) \rightarrow H^{1/2}(\Sigma) \times H^{-1/2}(\Sigma)$, is defined as the unique bounded linear operator satisfying $\gamma(\varphi) := (\gamma_D(\varphi), \gamma_N(\varphi)) := (\varphi|_\Sigma, \mathbf{n}_B \cdot \nabla \varphi|_\Sigma)$, $\forall \varphi \in \mathcal{C}^\infty(\overline{\Omega_B}) := \{\varphi|_\Omega, \varphi \in \mathcal{C}^\infty(\mathbb{R}^d)\}$, where \mathbf{n}_B is the unit normal on $\partial\Omega_B$ directed toward the exterior of Ω_B .

Next, denote \mathcal{G}_κ the outgoing Helmholtz *Green kernel* with wavenumber $\kappa > 0$, satisfying $(\Delta + \kappa^2)\mathcal{G}_\kappa = \delta$ in \mathbb{R}^d where δ is the Dirac delta function. For $d = 3$, $\mathcal{G}_\kappa(\mathbf{x}) := \exp(\iota\kappa|\mathbf{x}|)/(4\pi|\mathbf{x}|)$, and for $d = 2$ $\mathcal{G}_\kappa(\mathbf{x}) := \iota H_0^{(1)}(\kappa|\mathbf{x}|)/(4\pi)$, with $H_0^{(1)}$ the 0-th order Hankel function of the first kind [7, Chapter 9]. For any $\mathbf{x} \in \mathbb{R}^d \setminus \Sigma$, and sufficiently smooth traces (v, p) , define the *total layer potential operator* by

$$G_\Sigma(v, p)(\mathbf{x}) := \int_\Sigma \mathbf{n}_B(\mathbf{y}) \cdot (\nabla \mathcal{G}_\kappa)(\mathbf{x} - \mathbf{y}) v(\mathbf{y}) + \mathcal{G}_\kappa(\mathbf{x} - \mathbf{y}) p(\mathbf{y}) \, ds(\mathbf{y}), \quad (4)$$

where ds refers to the Lebesgue surface measure on Σ . The map $(v, p) \mapsto G_\Sigma(v, p)|_{\Omega_B}$ can be extended by density as a bounded linear operator $H^{1/2}(\Sigma) \times H^{-1/2}(\Sigma) \rightarrow H_{\text{loc}}^1(\Delta, \Omega_B)$. For any pair $(v, p) \in H^{1/2}(\Sigma) \times H^{-1/2}(\Sigma)$, the function $u := G_\Sigma(v, p)$ solves the Helmholtz equation with wavenumber κ in $\mathbb{R}^d \setminus \Sigma$, see e.g. [10, §3.1], and satisfies Sommerfeld's radiation condition, see [8].

Using the Dirichlet-Neumann trace map γ , we form the *Calderón projector* $\gamma \cdot G_\Sigma: H^{1/2}(\Sigma) \times H^{-1/2}(\Sigma) \rightarrow H^{1/2}(\Sigma) \times H^{-1/2}(\Sigma)$, commonly decomposed as

$$\gamma \cdot G_\Sigma = \frac{1}{2} \begin{bmatrix} \text{Id} & 0 \\ 0 & \text{Id} \end{bmatrix} + \begin{bmatrix} \mathbf{K}_\kappa & \mathbf{V}_\kappa \\ \mathbf{W}_\kappa & \check{\mathbf{K}}_\kappa \end{bmatrix},$$

where the four classical *Boundary Integral Operators* (BIOs) appear: $V_\kappa : H^{-1/2}(\Sigma) \rightarrow H^{1/2}(\Sigma)$ (*single layer*), $K_\kappa : H^{1/2}(\Sigma) \rightarrow H^{1/2}(\Sigma)$ (*double layer*), $\tilde{K}_\kappa : H^{-1/2}(\Sigma) \rightarrow H^{-1/2}(\Sigma)$ (*adjoint double layer*), and $W_\kappa : H^{1/2}(\Sigma) \rightarrow H^{-1/2}(\Sigma)$ (*hypersingular*). Both V_κ and W_κ are symmetric, while $K_\kappa^* = -\tilde{K}_\kappa$. We recall that the adjoint $*$ does not involve complex conjugation.

These BIOs naturally arise when deriving Boundary Integral Equations for Dirichlet or Neumann boundary conditions. For instance, for $u \in H^1(\Omega_B)$ such that $\Delta u + \kappa^2 u = 0$ in Ω_B , they appear in the *Calderón equations* (see [10, Sect. 3.4])

$$(\text{Id}/2 - K_\kappa)\gamma_D(u) = V_\kappa \gamma_N(u), \quad (5a)$$

$$(\text{Id}/2 - \tilde{K}_\kappa)\gamma_N(u) = W_\kappa \gamma_D(u). \quad (5b)$$

Alternatively, combinations of these BIOs arise when dealing with an outgoing impedance boundary condition $\mathbf{n}_B \cdot \nabla u|_\Sigma - \iota T_\Sigma u|_\Sigma = g$, $g \in H^{-1/2}(\Sigma)$. For instance, subtracting $\iota V_\kappa T_\Sigma \gamma_D(u)$ in Equation (5a) yields $D_{\kappa, T_\Sigma}^* \gamma_D(u) = V_\kappa(g)$, where we introduced the *impedance BIO* $D_{\kappa, T_\Sigma}^* := (\text{Id}/2 - K_\kappa) - \iota V_\kappa T_\Sigma$. Other impedance BIOs could be derived using the Calderón equation (5b), but we do not focus on them.

For particular values of κ , called *spurious resonances*, $V_\kappa, K_\kappa, \tilde{K}_\kappa$ and W_κ are well known to be singular [2, 7, 10]. A similar result holds for the impedance BIO D_{κ, T_Σ}^* , see [2, Sect. 2.6].

Lemma 1 *We have $\ker(D_{\kappa, T_\Sigma}^*) \neq \{0\}$ if and only if the homogeneous Dirichlet Helmholtz problem set in $\mathbb{R}^d \setminus \overline{\Omega_B}$ with wavenumber κ has a non-trivial solution. The elements of $\ker(D_{\kappa, T_\Sigma}^*)$ are the Dirichlet traces of solutions to Helmholtz problems set in Ω_B with non-homogeneous impedance boundary condition $g \in \ker(V_\kappa)$.*

Remark 1 Since Ω_B is a connected unbounded domain with bounded boundary, $\ker(V_\kappa) = \ker(\text{Id}/2 + \tilde{K}_\kappa) = \ker(D_{\kappa, T_\Sigma})$. When Ω_B is bounded, $\ker(V_\kappa) = \ker(\text{Id}/2 + \tilde{K}_\kappa) \neq \ker(D_{\kappa, T_\Sigma})$.

Because of spurious resonances, classical FEM-BEM formulations can be non-uniquely solvable at certain wavenumbers, even when (1) is well-posed, see [11]. The classical Johnson-Nédélec (JN) and Costabel couplings are of the form (3) by taking respectively

$$A_{\Sigma, \text{JN}} := \begin{bmatrix} 0 & \text{Id} \\ \text{Id}/2 - K_\kappa & -V_\kappa \end{bmatrix} \quad \text{and} \quad A_{\Sigma, \text{C}} := \begin{bmatrix} W_\kappa & \text{Id}/2 + \tilde{K}_\kappa \\ \text{Id}/2 - K_\kappa & -V_\kappa \end{bmatrix}.$$

We now establish that the GOSM reformulations (2) of these FEM-BEM formulations suffer from the same spurious resonances. Indeed, the inverse of $A_\Sigma - \iota B_\Sigma^* T_\Sigma B_\Sigma$ is needed to define S_B , but, due to spurious resonances, $A_\Sigma - \iota B_\Sigma^* T_\Sigma B_\Sigma$ can be singular. In the following proofs, note that $B_\Sigma^*(p) = (p, 0)$, so $B_\Sigma^* T_\Sigma B_\Sigma(\phi, p) = (T_\Sigma \phi, 0)$.

Proposition 1 (Johnson-Nédélec coupling) *If $A_\Sigma = A_{\Sigma, \text{JN}}$, then*

$$\ker(A_\Sigma - \iota B_\Sigma^* T_\Sigma B_\Sigma) = \{(\phi, \iota T_\Sigma \phi) \mid \phi \in \ker(D_{\kappa, T_\Sigma}^*)\}.$$

Proof. $(\phi, p) \in \ker(A_\Sigma - \iota B_\Sigma^* T_\Sigma B_\Sigma)$ if and only if $[-\iota T_\Sigma \phi + p = 0$ and $(\text{Id}/2 - K_\kappa)\phi - V_\kappa p = 0$], which is equivalent to $[p = \iota T_\Sigma \phi$ and $D_{\kappa, T_\Sigma}^* \phi = 0]$. \square

Proposition 2 (Costabel coupling) *If $A_\Sigma = A_{\Sigma, C}$, then*

$$\ker(A_\Sigma - \iota B_\Sigma^* T_\Sigma B_\Sigma) = \{(0, p) \mid p \in \ker(D_{\kappa, T_\Sigma})\}.$$

Proof. We first prove (C). Let $(\phi, p) \in \ker(A_\Sigma - \iota B_\Sigma^* T_\Sigma B_\Sigma)$. Then

$$(W_\kappa - \iota T_\Sigma)\phi + (\text{Id}/2 + \tilde{K}_\kappa)p = 0, \quad (\text{Id}/2 - K_\kappa)\phi - V_\kappa p = 0. \quad (6)$$

Let $w := G_\Sigma(\phi, p)$ and apply the Dirichlet-Neumann trace operator γ on w to obtain $\gamma_D(w) = (\text{Id}/2 + K_\kappa)\phi + V_\kappa p$ and $\gamma_N(w) = W_\kappa \phi + (\text{Id}/2 + \tilde{K}_\kappa)p$. It follows from Equation (6) that $\phi = \gamma_D(w)$ and $\gamma_N(w) = \iota T_\Sigma \phi$. The impedance trace $\gamma_N(w) - \iota T_\Sigma \gamma_D(w)$ is then null. Since by construction w is solution to the Helmholtz equation in Ω_B and satisfies Sommerfeld's radiation condition, $w = 0$, and so $\phi = 0$. Using T_Σ to combine the two equations of (6), we conclude that $p \in \ker(D_{\kappa, T_\Sigma})$.

To prove (D), observe that according to Remark 1, $p \in \ker(D_{\kappa, T_\Sigma}) = \ker(V_\kappa) = \ker(\text{Id}/2 + \tilde{K}_\kappa)$, so we directly obtain the relations in Equation (6) for $\phi = 0$. \square

Remark 2 Propositions 1–2 still hold when A_Σ is derived from a bounded domain, even though Remark 1 no more holds. The proofs are even simpler since $\ker(D_{\kappa, T_\Sigma}^*)$ and $\ker(D_{\kappa, T_\Sigma})$ are both reduced to the trivial element, so is $\ker(A_\Sigma - \iota B_\Sigma^* T_\Sigma B_\Sigma)$.

Remark 3 Most of the restrictions imposed on the geometry in Section 1 have been made to simplify the expression of the variational formulation (3), and those of the kernels in Propositions 1–2. The expressions of the kernels hold when Ω_B is still connected, but Ω_F is not connected or $\partial\Omega_O \not\subseteq \partial\Omega_F$ (see e.g. Figure 1 (right)), by taking care of considering $\partial\Omega_B$ instead of Σ .

3 Numerical illustration

We consider the scattering of an incoming plane wave $u_i(r, \theta) = \exp(\iota\kappa r \cos \theta)$, where (r, θ) are the polar coordinates, by a sound-soft obstacle $\mathcal{D} = \Omega_O$, which is a disk of radius 1. The whole domain $\Omega = \mathbb{R}^d \setminus \mathcal{D}$ is assumed homogeneous, that is, $\kappa = k > 0$ constant. This can be modeled by Problem (1) with (non-homogeneous) Dirichlet boundary conditions and $f = 0$, whose unique solution is

$$u_S(r, \theta) := - \sum_{p \in \mathbb{Z}} \exp(\iota p \theta) \iota^{|p|} J_{|p|}(\kappa) H_{|p|}^1(\kappa r) / H_{|p|}^1(\kappa),$$

with J_ν and H_ν^1 respectively the Bessel and Hankel function of first kind of order ν . Here, Ω_F is the annulus of radii 1 and 2, and $\Omega_B = \Omega \setminus (\overline{\Omega_F} \cup \overline{\Omega_O})$, see Figure 1 (left).

As transmission operator T_Σ in the BEM domain we choose $W_{i\kappa}$, the hypersingular operator for the *Yukawa operator*, that is, $-\Delta + \kappa^2 \text{Id}$. As transmission operator T_{Ω_F} in the FEM domain we choose a Schur complement-based operator relying on the discretization of a positive Dirichlet-to-Neumann map for the Yukawa operator, see [9, Chapter 8]. For more details about the expression of the chosen transmission operators, we refer to [1, Sect. 10.2]. We use \mathbb{P}_1 -Lagrange finite and boundary elements. Finite element (resp. boundary element) matrices are stored in sparse (resp. dense) format. For the sake of simplicity, for the discrete unknowns, we use the same notations as for the continuous unknowns. The numerical solution of the GOSM substructured formulation (2) is obtained using the GMRes method.

The spurious resonances for the considered geometry are the zeros of J_ν , divided by 2 (Ω_F is of radius 2), see e.g. [2, Th. 2.25]. We assume that κ is not a spurious resonance, so $A_\Sigma - \iota B_\Sigma^* T_\Sigma B_\Sigma$ is invertible. To illustrate the sensitivity or the robustness to spurious resonances of the GOSM for the JN and Costabel couplings, we study how the relative error of several quantities of interest evolves with respect to κ . We focus on the wavenumber range $\kappa \in [4.28, 4.42]$, inside which only $\kappa_1 \approx 4.32685$ and $\kappa_2 \approx 4.38575$ are spurious resonances. All the experiments have been led with a fixed mesh generated for $\kappa = 10$ and 20 points per wavelength.

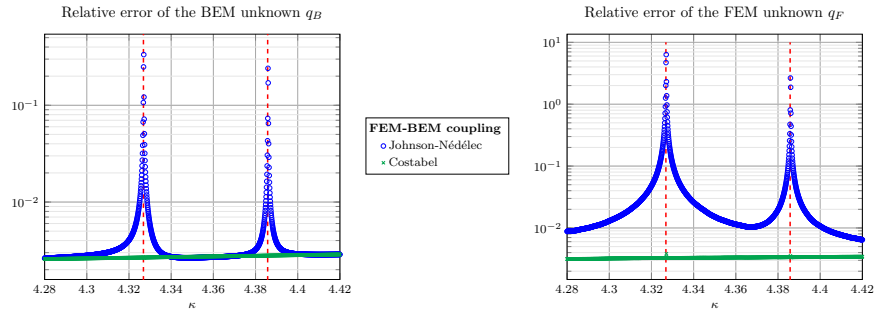


Fig. 2 Relative error of the BEM (left) and FEM (right) unknowns.

Our first quantity of interest is the BEM unknown q_B . In Figure 2 (left) we observe, for the JN coupling, peaks in the relative error of q_B when κ is close to the spurious resonances κ_1 and κ_2 . No peaks are observed in the curve associated with the Costabel coupling. These results may be interpreted given the explicit expressions of the coupling kernels stated in Propositions 1–2, and of the scattering operator S_B (see the end of Section 1). First, assume we want to compute $S_B q$ for a given vector q , and denote $v_q := (A_\Sigma - \iota B_\Sigma^* T_\Sigma B_\Sigma)^{-1} B_\Sigma^* q$. Because of the definition of B_Σ only the first component of v_q is relevant to compute $S_B q = q + 2\iota T_\Sigma B_\Sigma v_q$. Second, when κ is a spurious resonance only the second component of the eigenvectors of the Costabel operator $A_\Sigma - \iota B_\Sigma^* T_\Sigma B_\Sigma$ is non-trivial. Thus, when numerically inverting that operator near a spurious resonance, we can expect the first component of v_q to be of good accuracy, while the second might be less accurate. Turning to the eigenvectors

of the JN operator, both components are non-trivial, so both components of v_q might deteriorate (especially the first one).

Next, we study the relative error of the FEM unknown q_F , shown in Figure 2 (right). As for the BEM curve, we observe peaks around spurious resonances only when considering the JN coupling. Nonetheless, we emphasize that $A_{\Omega_F} - i B_{\Omega_F}^* T_{\Omega_F} B_{\Omega_F}$ is invertible, whatever the wavenumber. The reasoning used to explain the growth of the relative error of the BEM unknown q_B can not hold for q_F . This suggests that, near a spurious resonance, the poor quality of q_B makes also q_F less accurate. Remembering that q_F and q_B are the data shared between the FEM and BEM subdomains, that observation is not surprising.

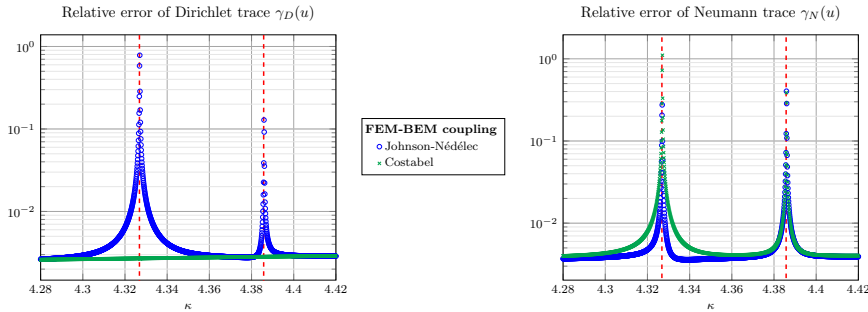


Fig. 3 Relative errors of reconstructed Dirichlet (left) and Neumann (right) traces.

We now turn to the evolution of the relative errors of $\gamma_D(u)$ and $\gamma_N(u)$, with respect to κ . We emphasize that $\gamma_D(u)$ and $\gamma_N(u)$ are *reconstructed* from the solution of the GOSM, namely $(\gamma_D(u), \gamma_N(u)) := (A_\Sigma - i B_\Sigma^* T_\Sigma B_\Sigma)^{-1} B_\Sigma^* q_B = v_{q_B}$. In Figure 3, when κ is close to a spurious resonance we observe peaks only in the Neumann relative error curve for the Costabel coupling, while there are peaks in both Dirichlet and Neumann curves for the JN coupling. The results confirm what we said previously about the deterioration near a spurious resonance of the components of v_q for a given vector q . It is interesting to note that the reconstructed solution $(\gamma_D(u), \gamma_N(u))$ is more and more spoiled when κ becomes closer to a spurious resonance, even though $A_\Sigma - i B_\Sigma^* T_\Sigma B_\Sigma$ is invertible. We highlight that the relative errors go from 1% to more than 100%, but are not comparable: around κ_1 the Dirichlet relative error is close to 1, while the Neumann relative error is close to 0.4. These two errors are too large for q_B and the reconstructed solution to be considered as good quality approximations.

We end by looking at Figure 4, which shows the relative error of u_F , the reconstructed volume solution in Ω_F , with respect to κ . We observe peaks around spurious resonances for the JN coupling, which are consequences of the peaks observed for q_F in Figure 2 (right). Moreover, it is coherent to recover an error for the solution in Ω_F for the JN coupling, because its Dirichlet trace should be equal to $\gamma_D(u)$, for which we have also observed a peak in the relative error. On the other hand, for the

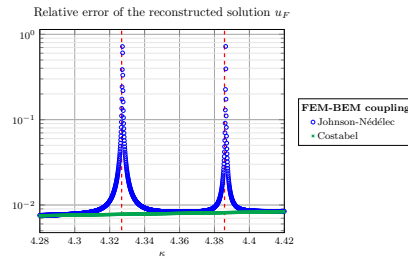


Fig. 4 Relative error of the reconstructed solution u_F in the FEM domain.

same reason, it is coherent to not observe any peak in the relative error when the Costabel coupling is used.

Finally, we pinpoint that relative errors peaks arise in the same way when classical FEM-BEM couplings (3) are considered. Indeed, for a geometry with two subdomains without an obstacle, it has been proven that only the Neumann component of the Costabel coupling can be spoiled, see for instance [11, Th. 1], while for the JN coupling both volume and Neumann components can be spoiled.

Acknowledgements This work is funded by the Inria program “Actions exploratoires” (OptiGPR3D).

References

1. Boisneault, A., Bonazzoli, M., Claeys, X., Marchand, P.: Discrete FEM-BEM coupling with the Generalized Optimized Schwarz Method. arXiv preprint arXiv:2601.16817 (2026)
2. Chandler-Wilde, S., Graham, I., Langdon, S., Spence, E.: Numerical-asymptotic boundary integral methods in high-frequency acoustic scattering. *Acta Numer.* **21**, 89–305 (2012)
3. Claeys, X.: Nonlocal optimized Schwarz method for the Helmholtz equation with physical boundaries. *SIAM J. Math. Anal.* **55**(6), 7490–7512 (2023)
4. Costabel, M.: Symmetric methods for the coupling of finite elements and boundary elements. In: *Mathematical and Computational Aspects*, pp. 411–420. Springer Berlin Heidelberg (1987)
5. Hiptmair, R., Meury, P.: Stabilized FEM-BEM coupling for Helmholtz transmission problems. *SIAM J. Numer. Anal.* **44**(5), 2107–2130 (2006)
6. Johnson, C., Nédélec, J.C.: On the coupling of boundary integral and finite element methods. *Math. of Comput.* **35**(152), 1063–1079 (1980)
7. McLean, W.C.H.: *Strongly elliptic systems and boundary integral equations*. Cambridge University Press (2000)
8. Nédélec, J.C.: *Acoustic and Electromagnetic Equations*. Springer New York (2001)
9. Parolin, E.: Non-overlapping domain decomposition methods with non-local transmission operators for harmonic wave propagation problems. Phd thesis, IP Paris (2020)
10. Sauter, S.A., Schwab, C.: *Boundary element methods, Springer Series in Computational Mathematics*, vol. 39. Springer-Verlag, Berlin (2011)
11. Schulz, E., Hiptmair, R.: Spurious resonances in coupled domain-boundary variational formulations of transmission problems in electromagnetism and acoustics. *Comput. Methods Appl. Math.* **22**(4), 971–985 (2022)